Journal of Applied Fluid Mechanics, Vol. 17, No. 7, pp. 1411-1429, 2024.
Available online at www.jafmonline.net, ISSN 1735-3572, EISSN 1735-3645.
https://doi.org/10.47176/jafm.17.7.2449

Hydraulic Investigation of Triangular Plan Form Vertical Drops

M. Abar, R. Daneshfaraz† and R. Norouzi

Department of Civil Engineering, Faculty of Engineering, University of Maragheh, Maragheh, East Azerbaijan, Iran

†Corresponding Author Email: daneshfaraz@maragheh.ac.ir

ABSTRACT

The vertical drop is one of the most widely used hydraulic structures for dissipating the destructive energy of water. The purpose of this research is to investigate the effect of the two difference height, and five vertex angles of a triangular plan form vertical drop on energy dissipation and average velocity using the volume of fluid (VOF) method. The findings revealed that by decreasing vertex angle of the triangular plan form vertical drop, energy dissipation increases. The lowest relative depth of the pool occurs with this drop. In contrast, as the vertex angle of the triangular plan form vertical drop decreases, the average velocity at the foot of the drop increases and the maximum average velocity in the triangular plan form vertical drop with an angle of 60 degrees and a height of 0.2 m is higher than other models. The average downstream velocity also decreases by decreasing the angle and this decrease is more intense in the center of the channel than on the sides.

Article History

Received November 22, 2023
Revised January 24, 2024
Accepted February 7, 2024
Available online April 30, 2024

Keywords:

Triangular plan form vertical drop
Energy dissipation
Relative depth of the pool
Average velocity

1. INTRODUCTION

Reducing the destructive energy of water in rivers and channels has always been an important concern of engineers. One of the most common energy consuming structures are drops. Vertical drops reduce the natural slope of the land to the design slope in areas that have a steep topographic slope and are mountainous. This structure consumes the kinetic energy caused by falling water on steep slopes, optimizes velocity in irrigation channels and networks, and transfers water from a higher level to a lower level with the least scouring of the bed (Daneshfaraz et al., 2019). The hydraulic performance of the drop is determined by hydraulic parameters such as energy dissipation, pool depth and downstream depth. These parameters are hydraulically dependent on each other, so that energy consumption increases with decreasing pool depth. The cases and purpose of using the drops are different in different regions, so that in some regions, high energy consumption is considered, and in others, water level control and regulation is considered. Actually, more energy dissipation in drops has always been considered by engineers, which is realized by different methods.

Most studies of vertical drops are related to the investigation of its hydraulic performace with a subcritical upstream flow. The first studies on vertical drops have been performed by Bakhmeteff (1932) who presented a relationship for the downstream water depth assuming hydrostatic pressure distribution, uniform velocity distribution, and conservation of energy. Other researchers, such as Moore (1943), White (1943), Rand (1955), Gill (1979), theoretically and experimentally investigated the hydraulic performance of vertical drops. In hydraulic research, parameters such as the relative depth of water downstream, the relative drop and the relative energy dissipation have been used, which respectively indicate the ratio of the water depth downstream of the drop to the height of the drop, the height of the drop and the ratio of energy dissipation to the height of the drop.

Chamani and Beirami (2002) investigated a vertical drop with upstream supercritical flow. Their results showed that for a fixed relative critical depth, relative energy dissipation, downstream relative depth, and relative depth of the pool increase with the decrease of the Froude number. Esen et al. (2004) placed a step with different dimensions downstream of a vertical drop with subcritical flow and investigated its effect on the hydraulic performance of the vertical drop. The results showed that the presence of a step increases the downstream relative water depth and the relative energy dissipation. They also found that by

NOMENCLATURE

ρ	water density	y_p	pool depth
μ	dynamic viscosity	y_1	downstream depth
g	gravitational acceleration	E_0	upstream total energy
h	drop height	E_1	Downstream specific energy
Q	flow discharge	ΔE	energy loss
y_0	upstream depth	σ	surface tension
y_c	critical depth	θ	vertex angle
y_b	brink depth		

increasing the relative height of the step, the relative downstream depth and energy dissipation increase.

Denli Tokyay and Yildiz (2007) studied the vertical drop with upstream supercritical flow. They were the first to calculate the splash length and splash depth caused by the impact of the jet onto the bottom of the pool. They also found that the relative depth of the pool depends only on the relative height of the drop.

Hong et al. (2010) experimentally investigated the effect of four different bottom slopes of the vertical drop on the hydraulic performance. The results of their investigation revealed that by increasing the downstream slope, the drop length and the impact force of the jet increase. Liu et al. (2014) investigated a drop with supercritical flow and an upstream floor slope. According to their results, the relative depth of the drop edge decreases with the increase of Froude number and the upstream slope.

Daneshfaraz et al. (2017) experimentally evaluated the effect of placement of screens with upstream supercritical flow on the energy dissipation. By increasing the Froude number, the relative energy dissipation increases and the efficiency of the screens is reduced. Also, a screen with a 50% porosity ratio and a distance of 125 cm from the gate showed superior performance.

Helmi et al. (2019) using the CFD method, they investigated the drop as a drop manhole, which is used to control the speed, reduce the slope and consume energy in sewer pipes. In this research, two drops have been used, the width of one is 3D and the other is D (D indicates the diameter). Their results showed that the maximum consumption of energy occurs in the drop in front of the inlet pipe and is 78 to 90 percent.

Daneshfaraz et al. (2020) studied the effect of horizontal double screens on the flow over a vertical drop edge with subcritical flow upstream. Findings showed increasing the relative length of the drop causes a decrease in the relative depth. The hydraulic performance of a vertical drop with three different heights, in the presence of a horizontal screen with two porosity ratios, was experimentally investigated by Daneshfaraz et al. (2021b). The results indicate that the use of a horizontal screen increases the relative depth of the pool, the relative downstream depth, and the relative energy dissipation. Also, the use of a horizontal screen in the vertical drop significantly reduces the downstream Froude number, and the increase in porosity of the horizontal screen reduces the wetted relative length of the horizontal screen and the relative mixing length.

Torres et al. (2021) labyrinth weir and Spillway were investigated using two software ANSYS Fluent and Open FOAM and with the physical model scale of Froude number 1:25. Their results showed that the standard k-ε turbulence model and the piecewise linear interface construction algorithm can predict the flow velocities and depths well. Also, this model is able to analyze the flow curve in the labyrinth weir at different flow levels, which is more accurate in low flow rates.

Norouzi et al. (2021) investigated the ability of artificial intelligence methods to evaluate energy dissipation in a vertical drop equipped with horizontal screens. The results show that the ANFIS_gbellmf method yields good performance in predicting hydraulic performance compared to other methods.

Daneshfaraz et al. (2022b) investigated the effect of a vertical downstream screen on a vertical drop, with different distances and porosities. They found that the presence of a vertical screen increases the downstream relative depth, the relative depth of the pool, and the relative energy dissipation. Daneshfaraz et al. (2022a) investigated a vertical drop using computational fluid dynamics. Their results indicated that by increasing the relative critical depth, the relative downstream depth, the relative depth of the pool, and the length of the drop increases and energy dissipation is reduced.

Yonesi et al. (2023) studied the energy dissipation in a vertical drop equipped with a horizontal screen at the edge with both smooth and rough downstream sections. According to their findings, at a relative critical depth greater than 0.3m, and with a vertical drop equipped with a screen and a rough bed, the length of the drop increases compared to a drop with a smooth bed. Daneshfaraz et al. (2023b) predicted the relative energy dissipation of a sloping drop equipped with a screen with two heights, three angles, and two different porosities using SVM and SVM-HHO methods. Their results showed that SVM-HHO method with RMSE=0.399, R^2=0.992, KGE=0.997 is more accurate than SVM method.

Crispino et al. (2023) the effect of a manhole with a supercritical bend with variable deflection angles and radius of curvature and different length of the straight element towards the downstream side on the hydraulic parameters

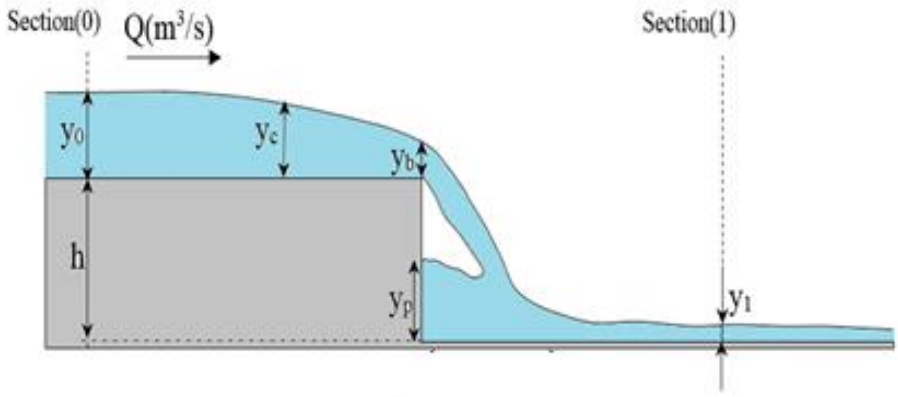

Fig. 1 Schematic of plain vertical drop

was investigated numerically. According to the results of this research, the hydraulic capacity of the curved manhole increases with the increase of the curvature radius and the length of the straight element, while the deflection angle does not have much effect.

According to the background of this research, studies have been carried out on the vertical drop along with the additional structure of the screen in different states or different states of the bottom or different types of flow in the upstream and the parameters of the relative depth of the downstream, the relative depth of the pool and relative energy dissipation have been investigated. In addition to the downstream relative depth parameters, relative pool depth and relative energy consumption, the present study has also examined the relative depth parameter of the brink with the triangulation plan of the vertical drop brink.

2. MATERIAL AND METHODS

In the present research, Chamani et al. (2008) was first verified using Flow 3D software, and then by applying innovation, the data obtained from the analysis of this software was presented in the present study.

2.1 Dimensional Analysis

In Fig. 1, the parameters affecting the energy dissipation are shown. The effective parameters for energy dissipation of the triangular plan vertical drop with sub-critical flow upstream are expressed in Eq. (1):

$$f_1(\rho,\mu,g,h,Q,y_0,y_c,y_b,y_1,y_p,E_0,E_1,\Delta E,\sigma,\theta)=0 \quad (1)$$

where ρ is the density of water [ML^{-3}], μ is the dynamic viscosity of water [$ML^{-1}T^{-1}$], g is gravitational acceleration [LT^{-2}], h is the drop height [L], Q is the flow discharge [L^3T^{-1}], y_0 is the depth upstream of the drop [L], y_c is the critical flow depth [L], y_b is the depth of water at the edge of the drop [L], y_p is the depth of the pool at the foot of the drop [L], y_1 is the downstream depth of water [L], E_0 is the total energy upstream of the drop [L], E_1 is the specific energy downstream of the drop [L], ΔE is the energy loss [L], σ is the surface tension [MT^{-2}], and θ is vertex angle of the triangular plan form vertical drop [dimensionless].

By using the π-Buckingham's method and considering h, g, ρ as repeated variables, dimensionless ratios are obtained according to Eq. (2):

$$f_2(Fr,\mathrm{Re},We,\frac{y_0}{h},\frac{y_c}{h},\frac{y_b}{h},\frac{y_1}{h},\frac{y_p}{h},\frac{E_0}{h},\frac{E_1}{h},\frac{\Delta E}{h},\theta)=0 \quad (2)$$

In Eq. (2), Fr is upstream Froude number, Re is upstream Reynolds number, We is the Weber number, $\frac{y_0}{h}$ is the relative initial depth, $\frac{y_c}{h}$ is the relative critical depth, $\frac{y_b}{h}$ is the relative depth at the edge, $\frac{y_1}{h}$ is the relative downstream depth, $\frac{y_p}{h}$ is the relative depth of the pool, $\frac{E_0}{h}$ is the relative energy upstream, $\frac{E_1}{h}$ is the relative energy downstream, and θ is the angle vertex of the drop.

Since the changes in the Froude number are insignificant (0.86 < Fr < 0.91), it can be ignored (Daneshfaraz et al., 2021a, 2023a). Also, due to the turbulence of the flow and the Reynolds number being in the range (153120 < Re < 338074), the effect of the Reynolds number is ignored (Bagherzadeh et al., 2022; Abbaszadeh et al., 2023). The Weber number is also negligible due to the sufficient water depth at the drop edge (Yonesi et al., 2023).

Factors affecting energy dissipation in the vertical drop are:

$$\frac{\Delta E}{E_0},\frac{\Delta E}{E_1}=f_3(\frac{y_0}{h},\frac{y_c}{h},\frac{y_b}{h},\frac{y_1}{h},\frac{y_p}{h},\theta) \quad (3)$$

The terms $\frac{\Delta E}{E_0},\frac{\Delta E}{E_1}$ in Eq. (3) are relative energy dissipation to the upstream and downstream of the drop, respectively.

The geometric and hydraulic specifications of the vertical drop are given in Table (1).

Table 1 Geometrical and hydraulic characteristics of plain and triangular plan vertical drop

Q (m^3/s)	B (m)	h (m)	θ(degree)	y_0 (m)	y_1 (m)	y_c (m)
0.021-0.0568	0.405	0.15 0.2	180	0.068-0.134 0.071-0.133	0.0313-0.0682 0.027-0.063	0.06495-0.126
		0.15 0.2	150	0.071-0.131 0.071-0.13	0.0318-0.0691 0.0268-0.0695	
		0.15 0.2	120	0.070-0.133 0.070-0.131	0.038-0.0718 0.035-0.670	
		0.15 0.2	90	0.069-0.13 0.070-0.13	0.037-0.076 0.044-0.072	
		0.15 0.2	60	0.068-0.129 0.069-0.125	0.041-0.101 0.05-0.098	

In Table (1), the width of the flume (B), the height of the drop (h), the flow discharge (Q) and its vertex angle (θ) are given. In addition, the downstream water depth limit (y_1) and the critical depth (y_c) are provided.

the Navier-Stokes equations and mass conservation with the finite volume method (Zahabi et al., 2018). Conservation of mass and Navier-Stokes equations are provided in Eqs. (4-7).

2.2 Governing Equations

Flow-3D software was used to simulate flow over the triangular plan form vertical drop. This software discretizes

$$V_F \frac{\partial \rho}{\partial t} + \frac{\partial(\rho u A_x)}{\partial x} + \frac{\partial(\rho v A_y}{\partial y} + \frac{\partial(\rho w A_z)}{\partial z} = R_{SOR} + R_{DIF} \quad (4)$$

$$\frac{\partial u}{\partial t} + \frac{1}{V_F}\left(uA_x \frac{\partial u}{\partial x} + vA_y \frac{\partial u}{\partial y} + wA_z \frac{\partial u}{\partial z}\right) = -\frac{1}{\rho}\frac{\partial P}{\partial x} + G_x + f_x \quad (5)$$

$$\frac{\partial v}{\partial t} + \frac{1}{V_F}\left(uA_x \frac{\partial v}{\partial x} + vA_y \frac{\partial v}{\partial y} + wA_z \frac{\partial v}{\partial z}\right) = -\frac{1}{\rho}\frac{\partial P}{\partial y} + G_y + f_y \quad (6)$$

$$\frac{\partial w}{\partial t} + \frac{1}{V_F}\left(uA_x \frac{\partial v}{\partial x} + vA_y \frac{\partial v}{\partial y} + wA_z \frac{\partial v}{\partial z}\right) = -\frac{1}{\rho}\frac{\partial P}{\partial z} + G_z + f_z \quad (7)$$

In these equations, (u,v,w) represent velocity components, (A_x,A_y,A_z) are the areas related to flow, (G_x,G_y,G_z) are mass accelerations, (f_x,f_y,f_z) refer to viscous forces, ρ is the fluid density, R_{SOR}, R_{DIF} are the turbulence diffusion terms, V_F is the volume associated with the flow, and P is the pressure.

2.3 The numerical Solution, Solution Network and Boundary Conditions

The numerical simulations will be compared with experiments from Chamani et al. (2008). Chamani et al. (2008) conducted their experiments in a flume with an 11-m length, a width of 0.405 m, a height of 0.7 m, and a drop height of 0.2 m.

Figure (2) shows the three-dimensional of a plain and triangular plan form vertical drop at different angles. The simulated length of the channel in the software is 4.5 m, the width is 0.405 m, and the length of the plain and triangular plan form vertical drop is 3 m at angles of 60, 90, 120 and 150 degrees.

The boundary conditions for the vertical drop are shown in Fig. 3. An inlet flow boundary condition is used for the channel inlet, a no-slip wall boundary condition for the walls and bottom of the channel, symmetry condition for the upper part of the channel and outlet flow boundary conditions for the end of the channel have been used.

It is necessary to choose the appropriate mesh size to get sufficiently accurate results. The optimal mesh size balances accuracy and numerical efficiency. Sometimes, to reduce the simulation time while increasing accuracy, two mesh blocks with different sizes can be used; these are called nested blocks. With this type of meshing, the mesh block with a smaller size is placed inside the mesh block with a larger size to obtain more detailed data in a region of the solution field (Bagherzadeh et al., 2022). According to Table 2, a suitable mesh size for this simulation has an element size of 0.015-0.0075 m with 1,108,080 elements.

In Table 2, the subscripts “exp” and “num” refer respectively, to experimental and numerical data. AE and RE% errors represent the absolute error (Eq. 8) and the percentage of relative error (Eq. 9) which are:

$$AE = \left| X_{\exp} - X_{num} \right| \quad (8)$$

$$RE(\%) = \left| \frac{X_{\exp} - X_{num}}{X_{\exp}} \right| \times 100 \quad (9)$$

Here X_{exp} is the experimental data and X_{num} is the data obtained from the numerical solution (Abbaszadeh et al., 2023).

The way to define the mesh in the software and the scope of the computational mesh in each of the mesh blocks are shown in Fig. 4. According to the figure, the mesh of the first block has 0.015 m elements and covers the entire channel, and the mesh of the second block starts from a distance 2 m from the beginning of the channel and the elements there have a size of 0.0075 m and extend to a distance of 4m.

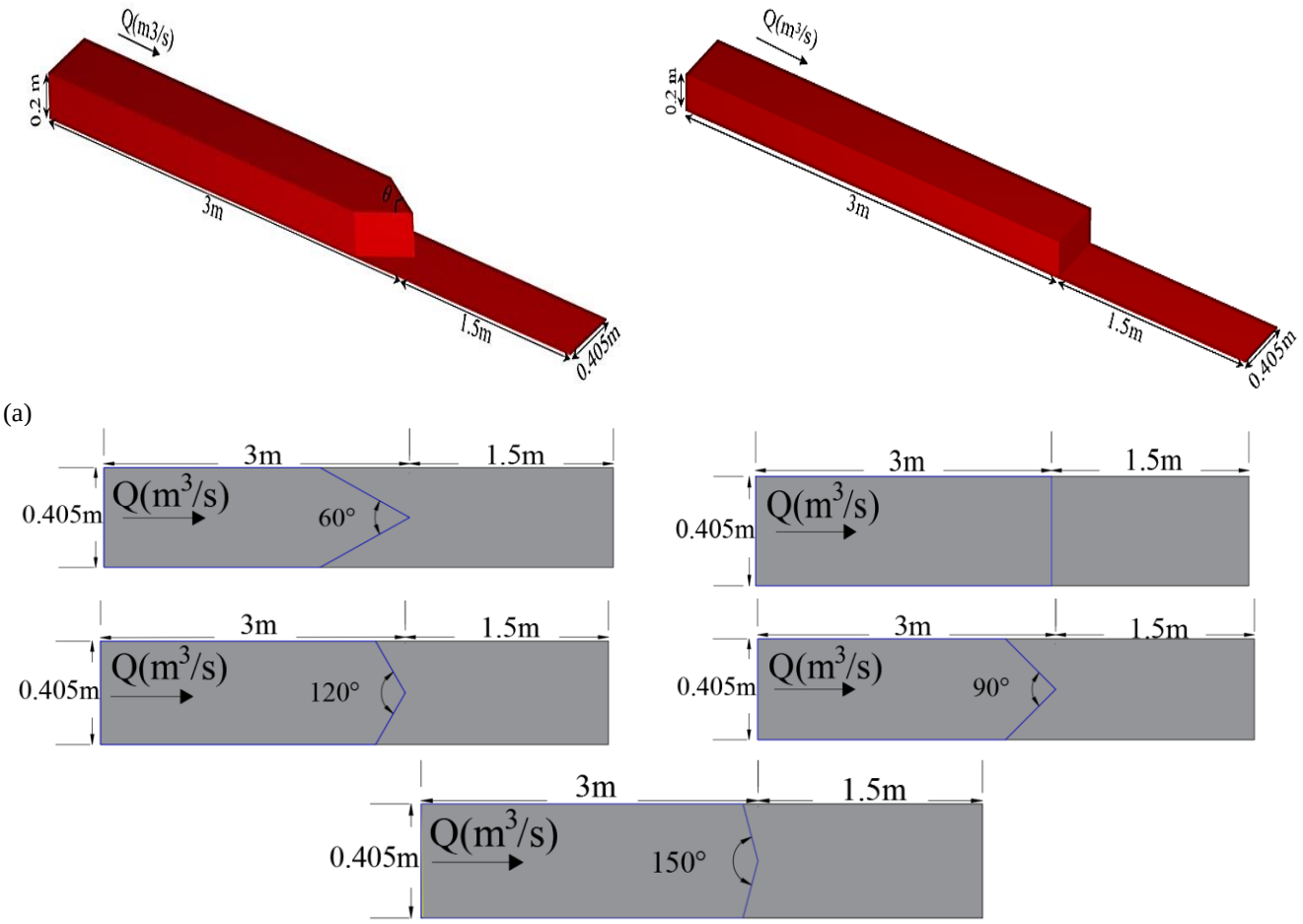

Fig. 2 (a) 3D view of plain and triangular plan vertical drop and (b) plan view of plain and triangular plan vertical drop with different vertex angles

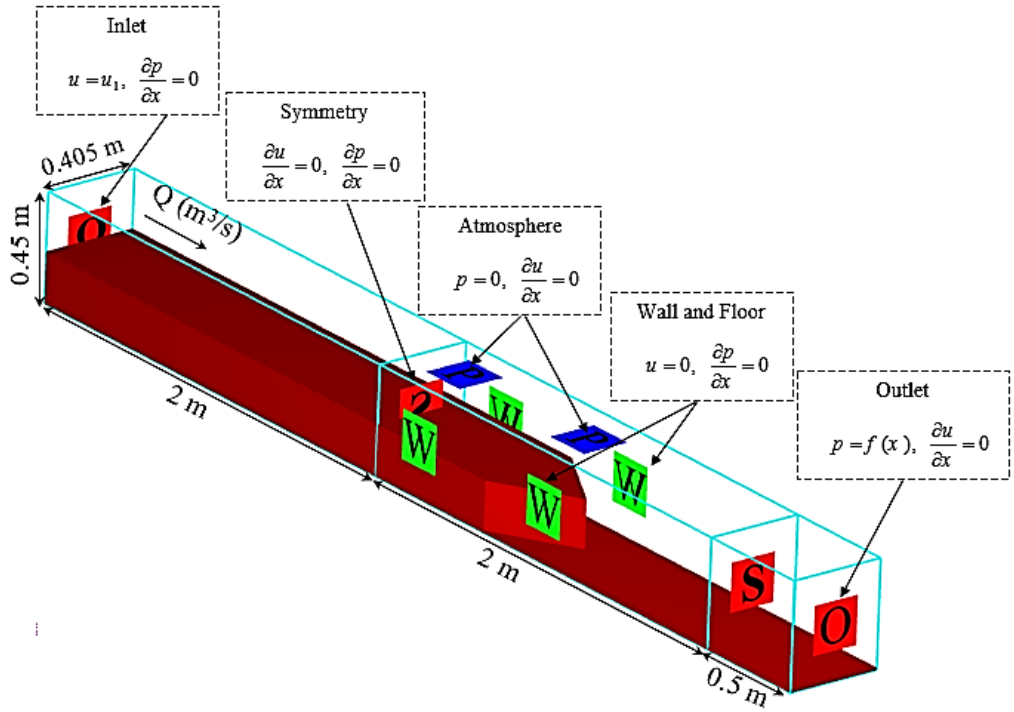

Fig. 3 Boundary conditions for vertical drop in Flow-3D software

Table 2 Results from mesh independence study

Model number	Q(m^3/s)	Size of cell	Number of cells	$(y_1)_{exp}$	$(y_1)_{num}$	AE(y_1)	RE(y_1)%
1	0.021	0.02-0.01	468000	0.025	0.0277	0.00266	10.66
2		0.015-0.0075	1108080		0.0272	0.00221	8.83
3		0.01-0.0055	3039002		0.275	0.00246	9.84
4		0.009-0.005	4041000		0.0279	0.00287	11.46
5		0.008-0.004	7261072		0.0273	0.00231	9.23

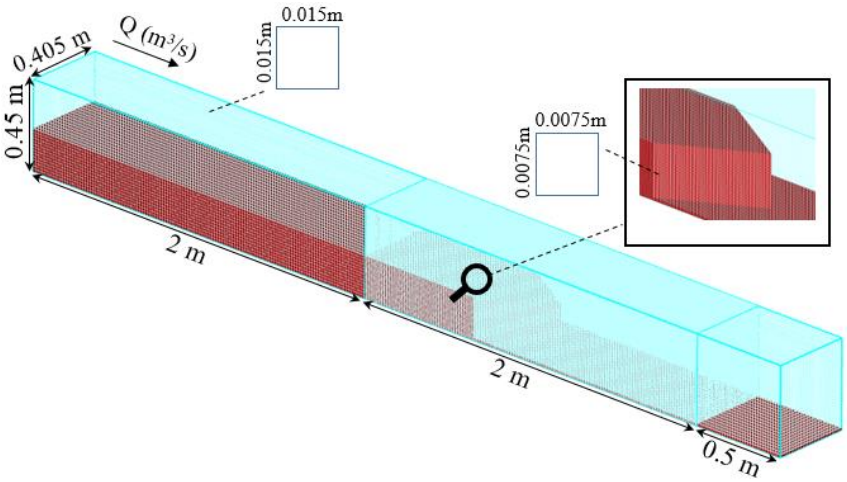

Fig. 4 Vertical drop grid

Table 3 Determination of turbulence model

	RNG	k-w	k-e	LES
Q(m^3/s)	0.021	0.021	0.021	0.021
$(y_1)_{exp}$	0.025	0.025	0.025	0.025
$(y_1)_{num}$	0.0272	0.0285	0.0273	0.0278
AE(y_1)	0.0022	0.0034	0.0022	0.0028
RE(y_1)%	8.83	13.9	8.98	11.19

According to Table 3 results from various turbulence models are shown. It can be seen that the RNG turbulence model has the lowest error compared with 0.22% and 8.83% absolute and relative error, respectively. Therefore, the RNG turbance model was chosen for further simulation and verification.

After determining the optimal mesh and choosing the turbulence model, validation of the numerical calculations was performed. Results from the calibration study are listed in Table 4.

The agreement bewteen simulated and measured data can be shown graphically as in Fig. 5. As can be seen, the correlation coefficient of this simulation is 0.9921 which indicates the excellent agreement. Calculation of the correlation coefficient is provided by Eq. (10).

$$R^2 = \left(\frac{n\sum X_{exp} X_{num} - (\sum X_{exp})(\sum X_{num})}{\sqrt{n(\sum X_{exp}^2) - (\sum X_{exp})^2}\sqrt{n(\sum X_{num}^2) - (\sum X_{num})^2}} \right)^2 \quad (10)$$

Table 4 Validation and calibration of numerical solution

Q(m^3/s)	$(y_1/h)_{exp}$	$(y_1/h)_{num}$	AE(y_1/h)	RE(y_1/h) %
0.021	0.125	0.136	0.011	8.83
0.0311	0.176	0.185	0.0093	5.27
0.0417	0.226	0.241	0.0151	6.7
0.0518	0.2755	0.293	0.0175	6.35
0.0568	0.3125	0.316	0.004	1.27

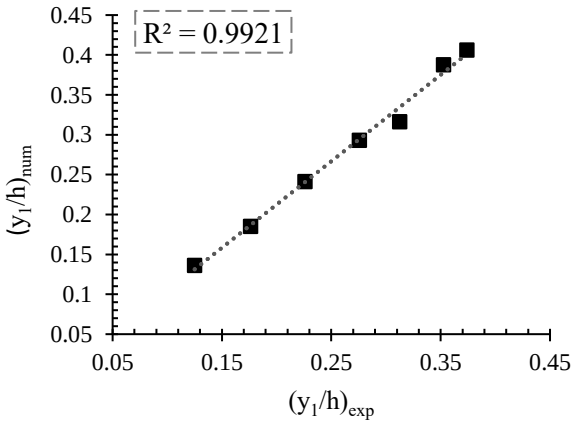

Fig. 5 Correlation between experimental and numerical results

2.4 Energy Dissipation in a Vertical Drop

Energy dissipation begins with a calculation of the upstream energy head at section 0, from Eq. (11).

$$E_0 = h + y_0 + \frac{q^2}{2gy_0^2} \tag{11}$$

Here, E_0 is the upstream total energy head, h is the height of the drop, y_0 is the upstream depth, q is the flow rate per unit width, and g is gravitational acceleration. Downstream water energy head can be calculated using:

$$E_1 = y_1 + \frac{q^2}{2gy_1^2} \tag{12}$$

where, E_1 is the downstream energy head and y_1 is the downstream depth at section 1. Next, energy dissipation and relative energy dissipation between locations 0 and 1 can be calculated from Eqs. (13) and (14), respectively:

$$\Delta E = E_0 - E_1 \tag{13}$$

$$\frac{\Delta E}{E_0} = \frac{E_0 - E_1}{E_0} \tag{14}$$

To calculate the efficiency (η) for energy dissipation of the vertical drop with a triangular plan edge compared to the plain vertical drop, Eq. (15) is used.

$$\eta = \frac{\Delta E_{(Triangular\ drop)}}{\Delta E_{(Plain\ drop)}} - 1 \tag{15}$$

3. RESULTS AND DISCUSSION

In this research, the effect of the height and vertex angle of a triangular plan form vertical drop on energy dissipation, depth of the drop edge, pool depth, depth of the downstream, and average flow velocity are discussed.

3.1 The influence of the Drop Vertex Angle on Energy Dissipation

Energy dissipation is caused by the impact of the flow jet with the floor and the creation of a pool with swirling currents. The drop vertex angle (in addition to the impact of the jet and the swirling currents in the pool, and the increase in the length of the edge) increases turbulence in the flow and also increases the energy dissipation.

According to Fig. 6, by reducing the drop vertex angle from 180 degrees to 150, 120, 90 and 60 degrees, the length of the drop wing has gradually increased, and the depth of the pool decreases, which causes an increase in energy dissipation. The greatest energy dissipation occurs with an angle of 60 degrees, which is 50.3% at a height of 0.15 m and 64.3% at a height of 0.2 m, for the lowest flow rate (0.021m3/s).

At the lowest flow rate, the intensity of the jet impact is greater and as a result, the energy dissipation is higher. At high flow rates, due to the increase in the volume of water entering the channel, the jet flow hits the pool instead of the bottom of the channel and causes energy dissipation.

From the flow lines passing over the drop, we can see the turbulence caused by the increase in the height of the vertical drop. The impact of the jet stream on the bottom of the channel affects the flow patterns and energy dissipation

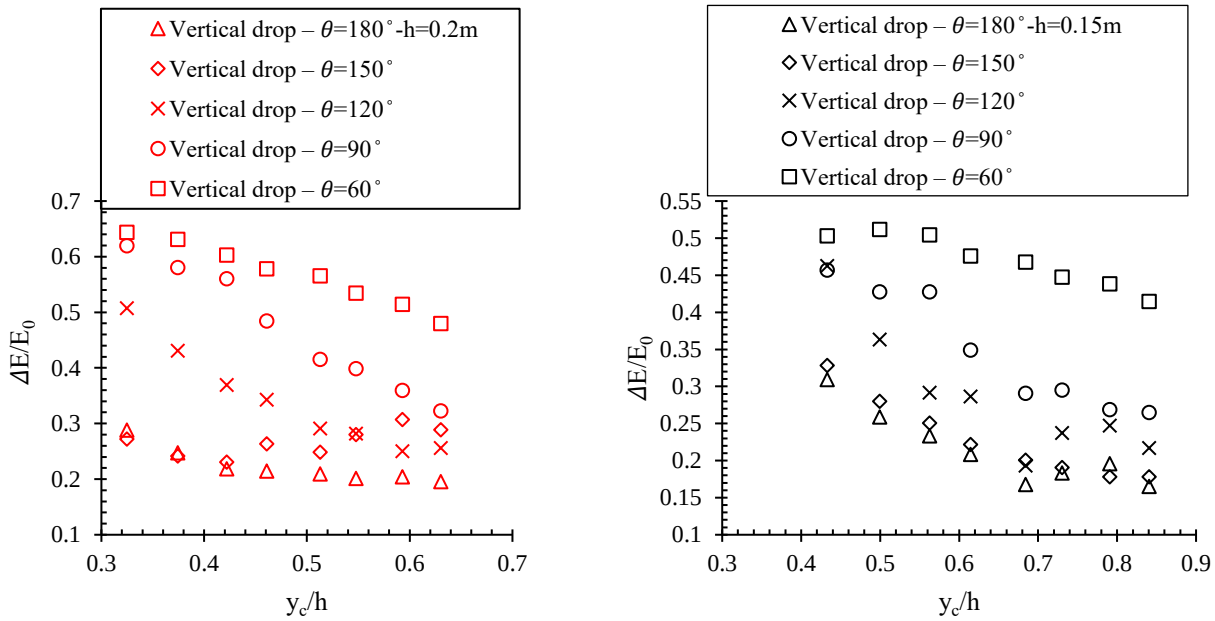

Fig. 6 Relative energy dissipation for a drop with height of 0.2 and 0.15 m

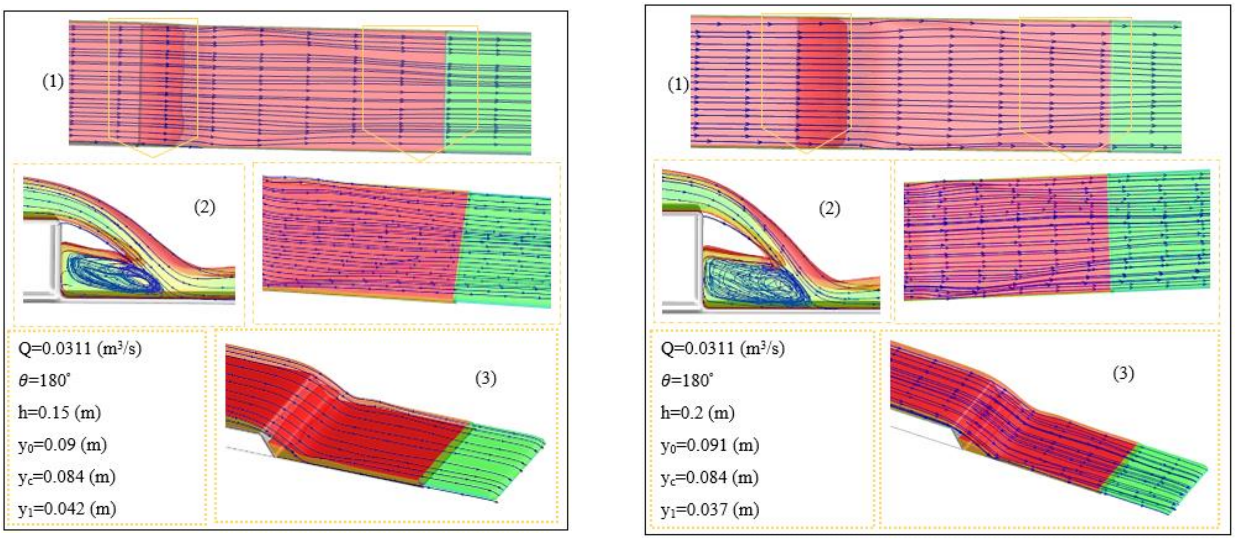

(a) (b)

Fig. 7 Flow lines passing over a vertical drop with: a) height of 0.15 m, b) height of 0.2 m

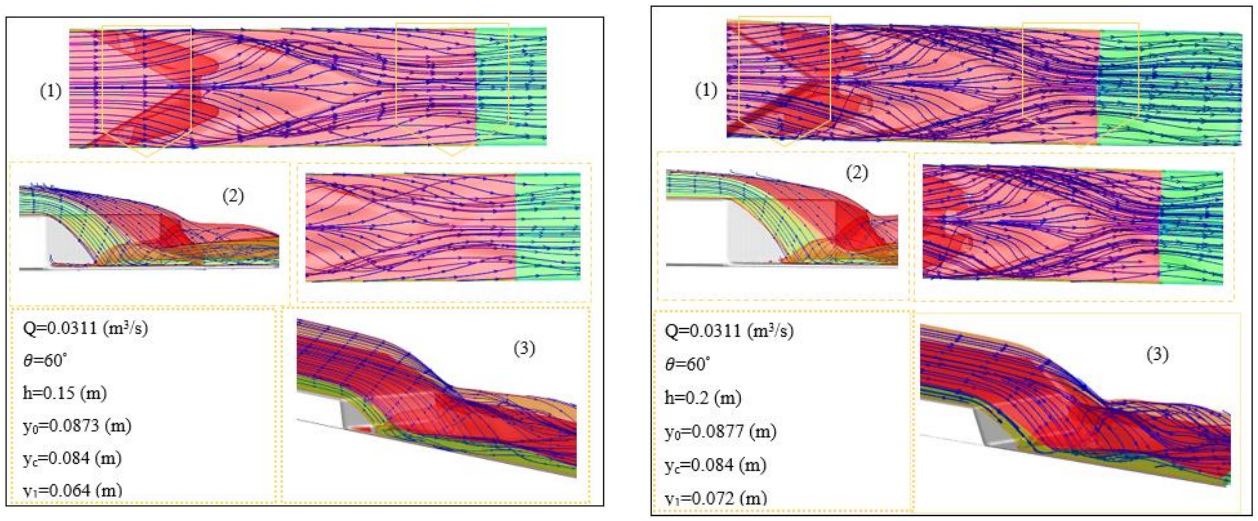

(a) (b)

Fig. 8 Flow lines over a vertical drop with vertex angle of 60 degrees with: a) a height of 0.15 m, b) a height of 0.2 m

within the pool. Turbulence and swirling currents increase the energy dissipation. Figure 7 illustrates the flow lines for a height of 0.15 m and 0.2 m and a flow rate of 0.0311 m^3/s. As can be seen, the flow upstream of both drops is uniform and unidirectional. But in the pool, the flow lines indicate circulation, eddies and turbulence. By comparing Fig. 7-a and 7-b, the turbulent and rotating flow in the pool for a drop of 0.2 m is more intense than for a drop of 0.15 m, providing a probable physical mechanism for the results. According to the figure, the plan view is shown with number (1), the longitudinal section is shown with number (2) and the three-dimensional view is shown with number (3).

The influences of the vertex angle and the height of of the triangular plan form vertical drop on the flow lines and energy dissipation are shown in Fig. 8. By comparing Fig. 7 and 8, it can be seen that the turbulence of the flow and consequently the energy dissipation in the pool, upstream and downstream of the vertical drop in Fig. 8 due to the length of drop wing, is greater than in the Fig. 8. It indicates more energy dissipation in the triangular plan form vertical drop compared to the plain vertical drop.

According to Fig. 8-a and 8-b, by the increasing in the height of the drop, the intensity of the impinging jet with a height of 0.2 m increases and as a result the turbulence increases.

Among the vertex angles of the drop, the angle of 60 degrees has the highest energy dissipation, therefore, the

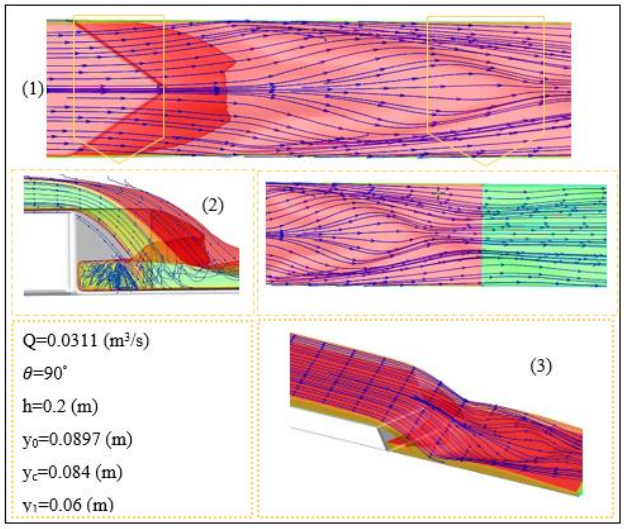

(a) Flow lines with a 90 degree vertex angle

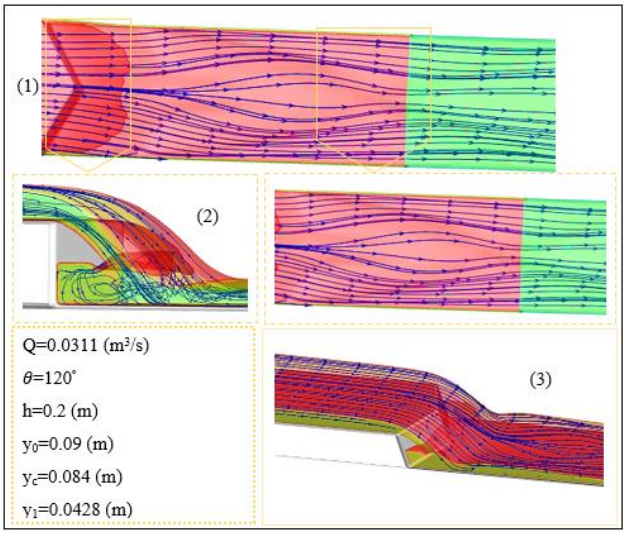

(b) Flow lines for a 120 degree vertex angle

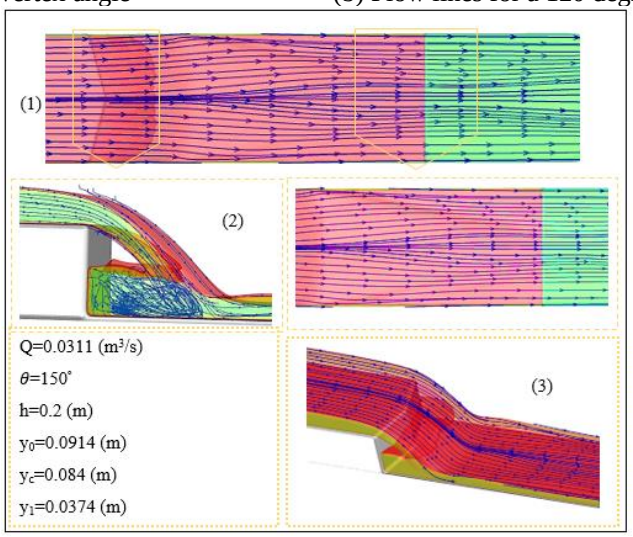

(c) Flow lines with an angle of 150 degrees

Fig. 9 Flow lines for a height of 0.2 m

flow lines for both heights of the drop are presented at this angle for a better comparison. The flow lines for vertex angles of 90, 120 and 150 degrees are presented for a 0.2 m drop. These cases lose more energy than drops at the same angles with a height of 0.15 m.

Figure 9 shows the flow lines of 90, 120 and 150 degree angles and a height of 0.2 m. It is seen that the flow lines are together downstream of the drop. The curvature, change of direction, and proximity of the flow lines is less than in Fig.8. Also, by reducing the angle from 150 to 120 and 90 degrees, the turbulence increases and as a result, energy dissipation increases.

3.2 The effect of the Drop Vertex Angle on the Depth of the Drop Brink

The depth of water at the drop edge in a plain drop is equal at different sections across the width, but when the brink becomes angled, according to the data taken at three points across the brink of the drop, at a distance of 0.1 meters from the walls in the wings and at a distance of 0.2025 meters from the wall, i.e. at the vertex the depths of the brink at the wing and the vertex angle are different. In Fig. 10, the relative depth at the drop edge decreases as the angle decreases from 150 degrees to 60 degrees. The minimum depth occurred with an angle of 60 degrees and at a flow rate of 0.021 m^3/s. At the drop wings, the brink depth is greater than the brink depth at the vertex angle. The reason for this is that the volume of water passing through the drop wing is greater than at the vertex angle, which happened due to the length of the brink.

In Fig. 11, the comparison of the drop brink depth of the plain drop and triangular plan form vertical drops at two sections: the vertex angle and its wing at two heights of the drop are shown. According to Fig. 11-a and c, the relative drop brink depth at the vertex angle is less compared to the relative depth of the wing in plain mode with the reduction of the vertex angle, but in Fig. 11-b and d the relative depth at the wing is compared to the relative drop brink depth

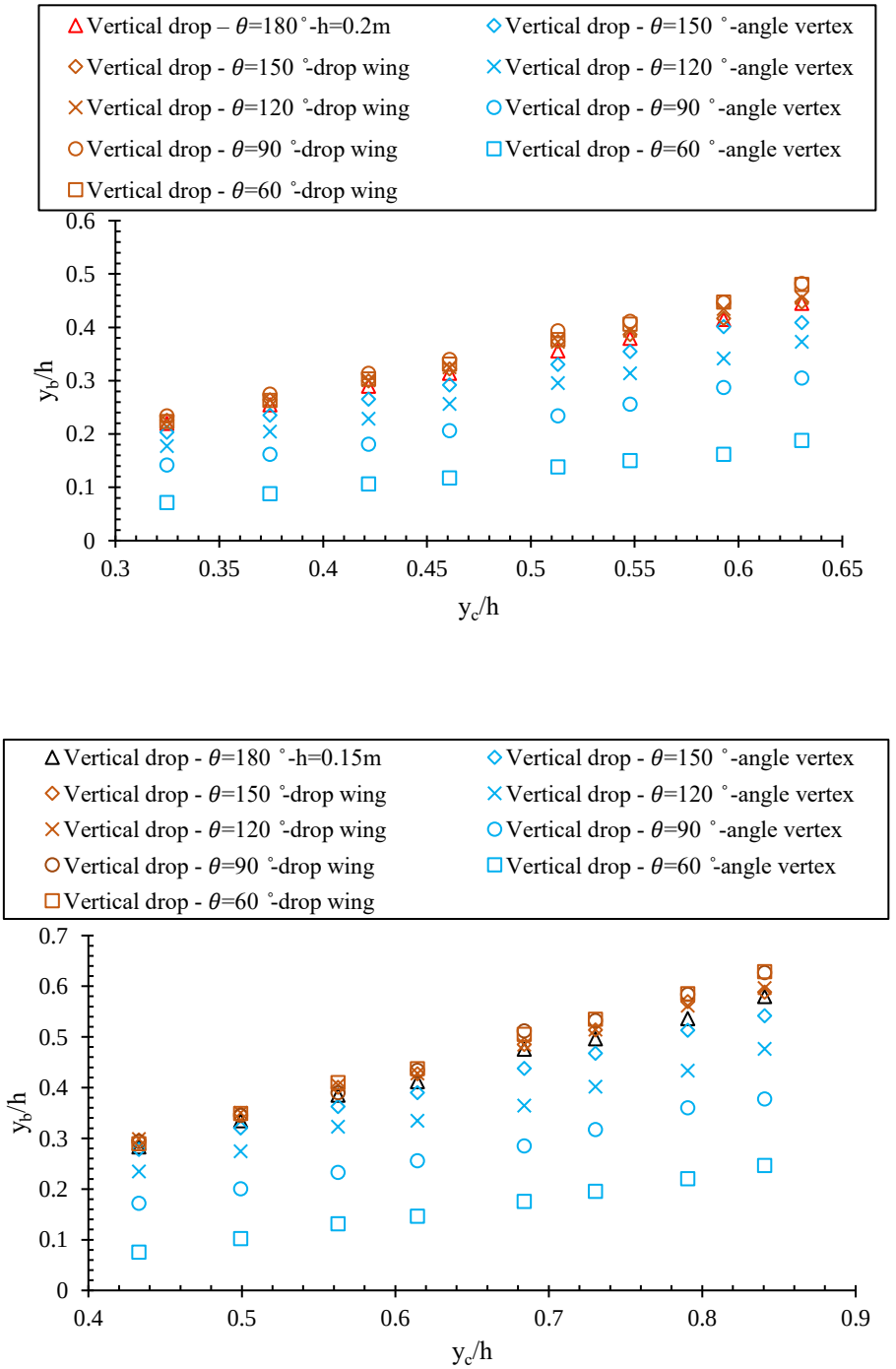

Fig. 10 Comparison of the changes in the relative depth of the drop brink at the vertex and wings with the decrease of the angle at two drop heights

in the plain case. The two depths are almost equal. Also, the relative drop brink depth for a 0.15m drop exceeds that for a 0.2m drop.

3.3 The Effect Of The Drop Vertex Angle On The Pool Depth

According to Fig. 12, increasing the critical depth means increasing the turbulence in the pool. Turbulence causes the depth of the pool to increase. Also, the pool depths at the foot of the angle vertex and at the wings are not equal, the relative pool depths at the foot of the two wings are equal and are different from that one at the angle vertex. According to Fig. 12-a, at the leading angle vertex with a height of 0.15 m, the angles of 90, 120, and 150 degrees lead to greater relative pool depth by 118%, 113%, and 114%, respectively, compared to the plain

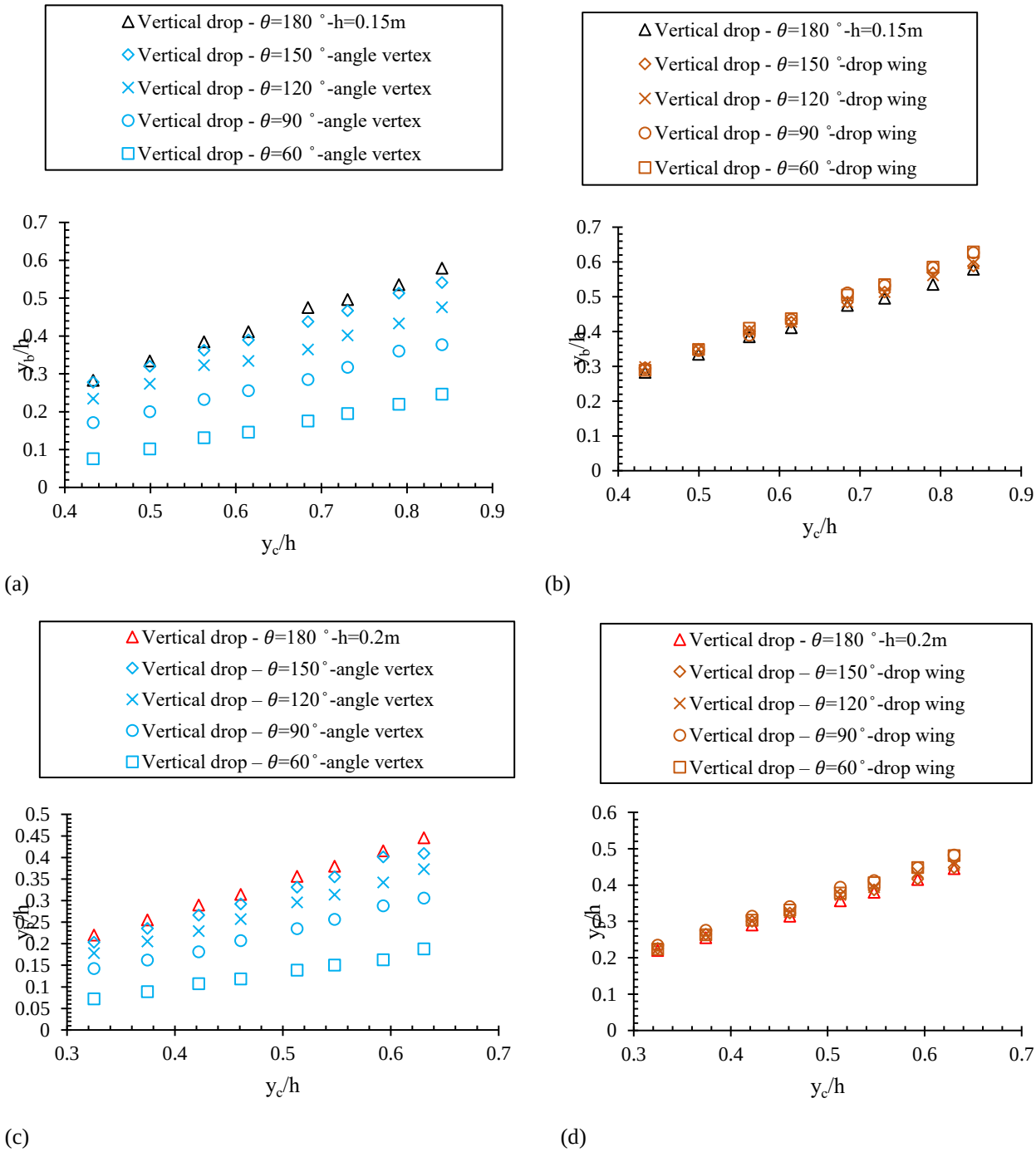

Fig. 11 The drop brink depth compared to the critical depth in the drop at a height of 0.15 and 0.2 m, respectively: a) relative depth of the brink at theangle vertex, b) relative drop brink depth at the wings, c) relative depth of the brink At the angle vertex, d) the relative drop brink depth at the wings

vertical drop. According to Fig. 12-b, at the foot of the drop, the relative pool depth decreases with the decrease of the angle vertex, and for the angles of 60, 90, 120 and 150 degrees, it is respectively decreased by 17.5%, 56.7%, 94.5% and 96.5%. the relative pool depth is the highest with a plain drop. In Fig. 12-c and d, the drop for a height of 0.2 m also has a similar trend as the drop with a height of 0.15 m.

3.4 The influence of the drop vertex angle on the downstream depth

The downstream water depth depends on the type of drop and upstream conditions. According to Fig. 13-a, the relative downstream water depth increases by decreasing the drop vertex angle from 180° to 60°. The reason for this is the increase in the length of the drop wing, which happens with

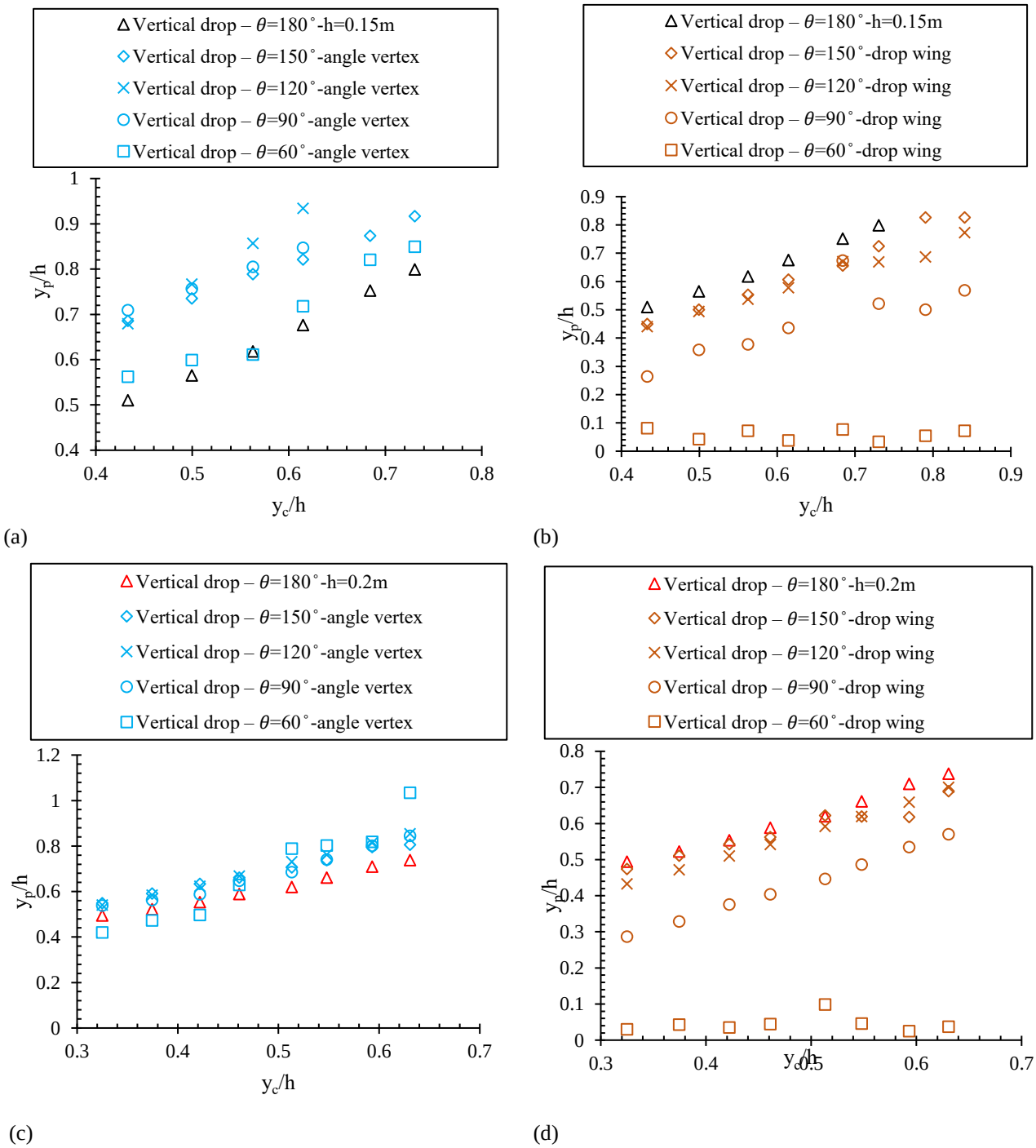

Fig. 12 The relative pool depth at two heights of the drop in: a-c) the angle vertex , b-d) the drop wing

the decrease of the angle vertex. In this way, the amount of water passing through the edge of the drop has increased, which causes the relative depth of the downstream to increase. The downstream depth of the drop at a height of 0.15 m, at an angle of 60 degrees and a relative critical depth of 0.68 has increased by 159% compared to a plain drop, as well as a vertical drop at a height of 0.2 m, at an angle of 60 degrees and a relative critical depth 0.51 has increased by 213% compared to the plain drop.

The Frude number downstream of the drop has also decreased at an angle of 60 degrees, so that with a 0.15m drop, it has decreased from 2.5, to 2.98, to 1.3, then to to 2

Also for a 0.2m drop, the Froude number range changed from 2.8- 3.7 to 0.99-1.5. The influence of the height of the drop on the relative downstream depth is such that the drop with a lower height has a greater relative downstream depth. According to the Fig. 13-b, with attention to the relative downstream depth and also to the the flow downstream of

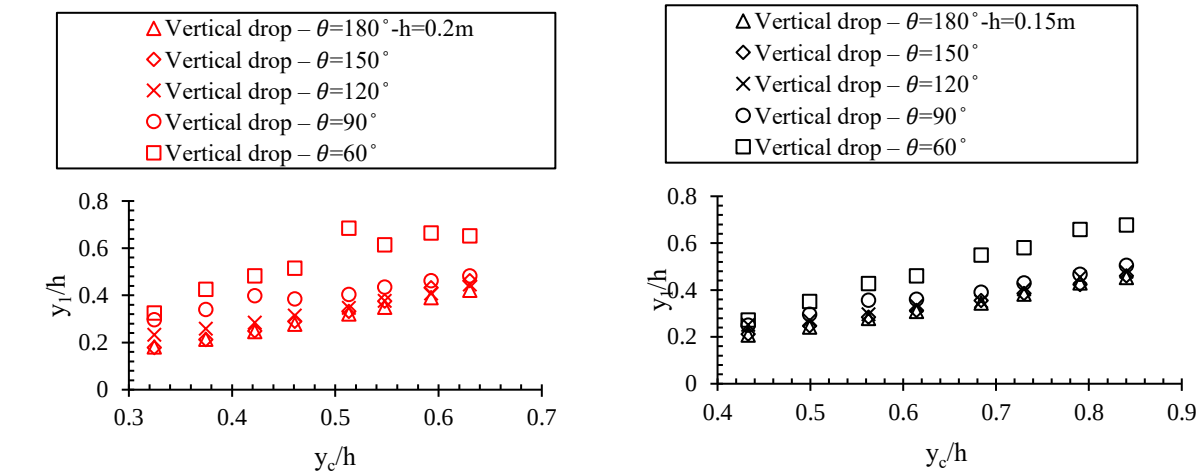

(a)

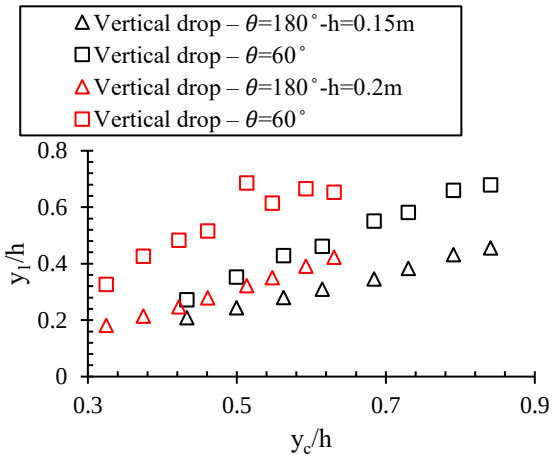

(b)

Fig. 13 Changes in the relative downstream depth at different vertex angles with the height of the drop 0.15 and 0.2 m

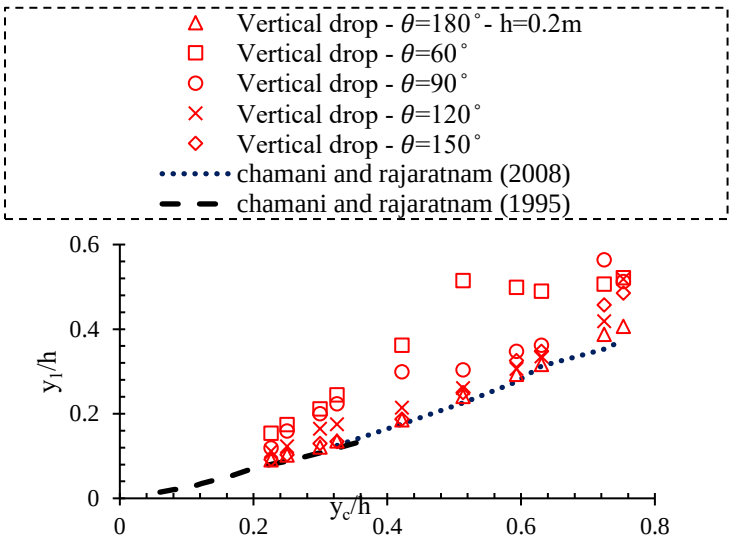

Fig. 14 Comparing the research of previous researchers with the results of the current research

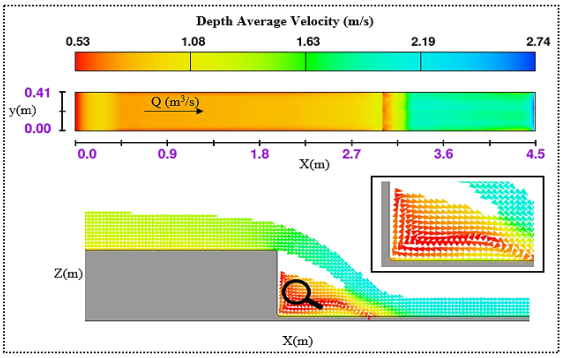

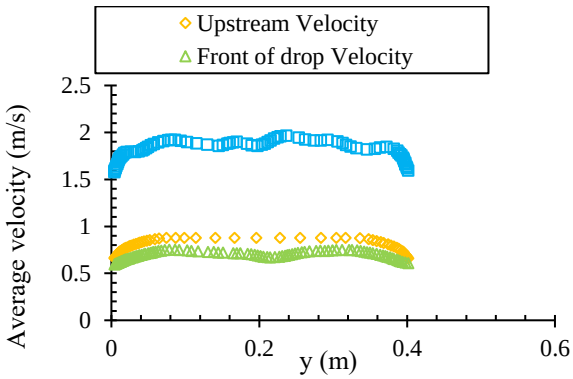

(a) Plain drop with a height of 0.15 m

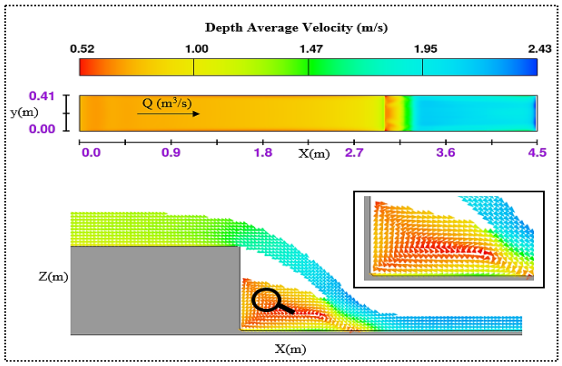

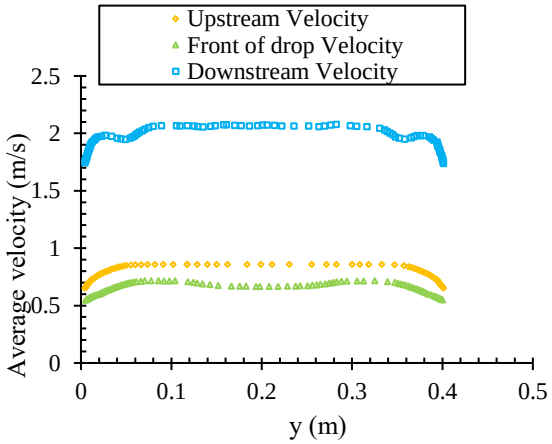

(b) Plain drop with a height of 0.2 m

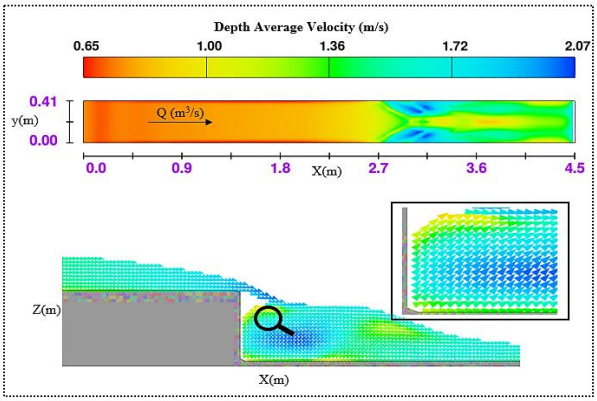

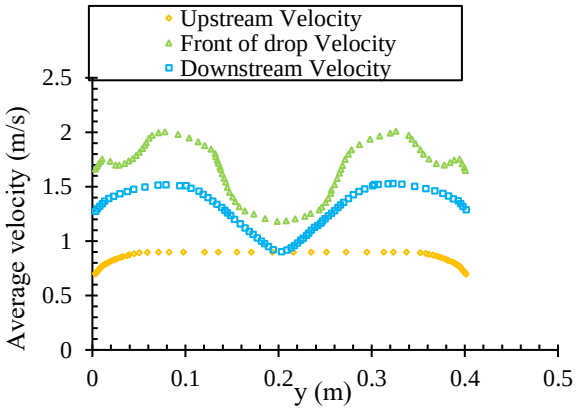

(c) Drop with vertex angle of 60 degrees and a height of 0.15 m

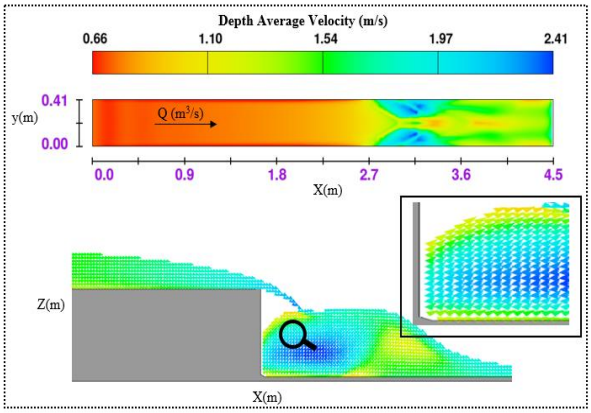

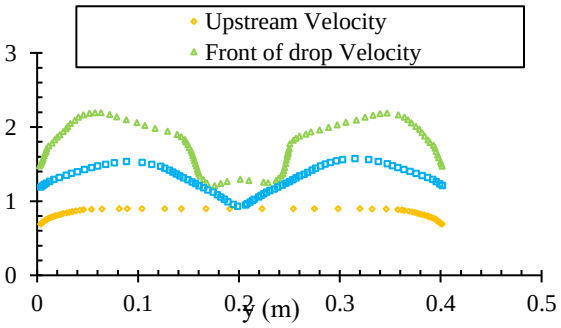

(d) Drop with a vertex angle of 60 degrees and a height of 0.2 m

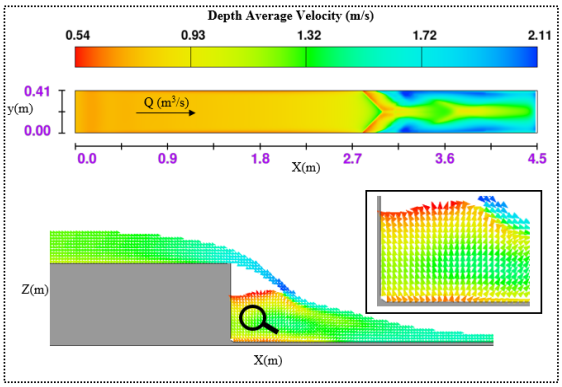

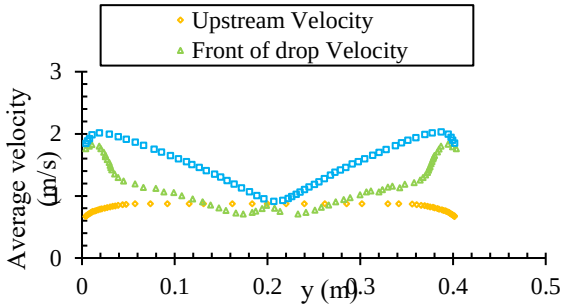

(e) Drop with a vertex angle of 90 degree and a height of 0.2 m

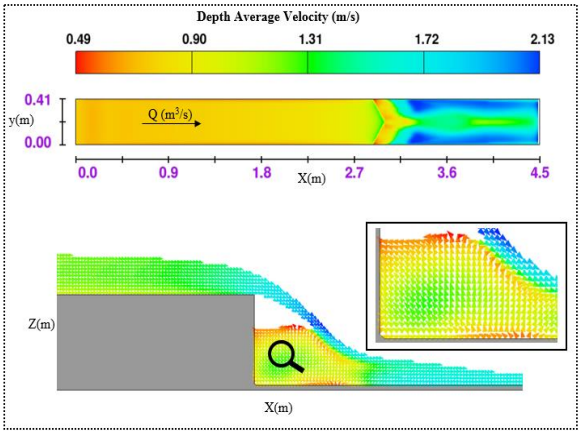

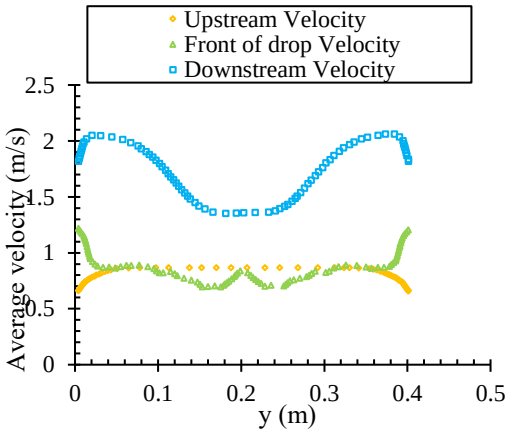

(f) Drop with a vertex angle 120 degree and a height of 0.2 m

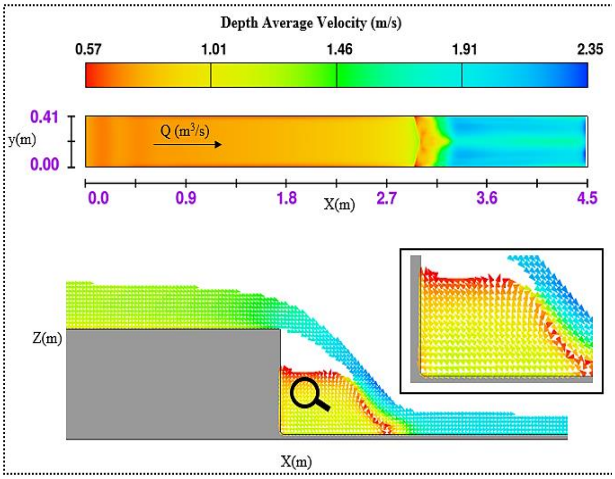

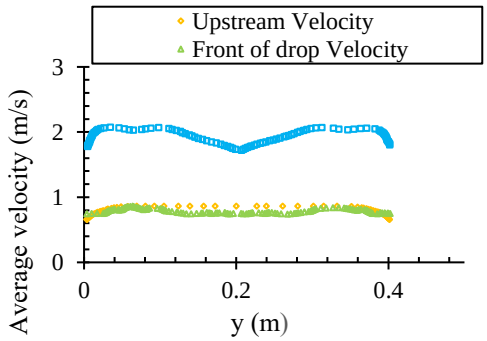

(g) Drop with the vertex angle of 150 degrees and a height of 0.2 m

Fig. 15 Average velocity at different sections of the drop

the drop with a height of 0.2 m, with an angle of 60 degrees is favorable.

In order to check the accuracy of the results obtained from the current research, the relative depth of the downstream in the drop of the triangular plan with different angles has been compared with the relative depth of the downstream of the studies of other researchers, according to Fig. 14.

3.5 The Effect of the Drop Vertex Angle on the Flow Velocity Across the Channel

The velocity of the flow passing over the drop is one of the most important hydraulic parameters to control the flow and prevent possible damages. In Fig. 15, the average velocity of the flow at different sections of the channel width, (upstream of the drop, at the foot of the drop (in front of the vertex angle) and downstream of the drop) can be seen. Figure 15-a and b show the average velocity of a

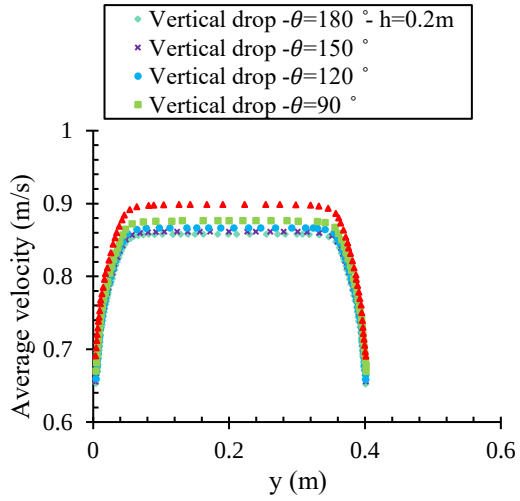

a) Average velocity upstream of the drop

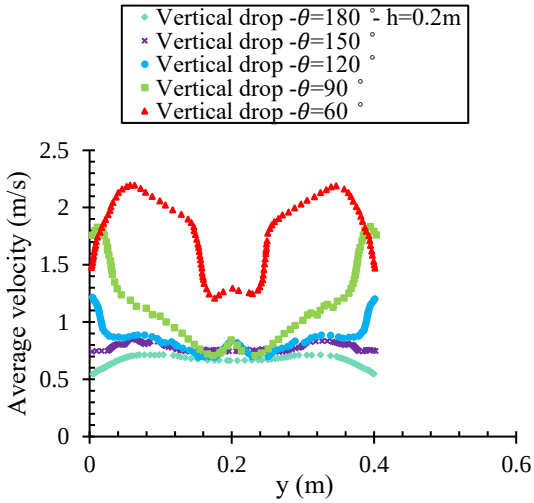

b) Average velocity at the foot of the drop

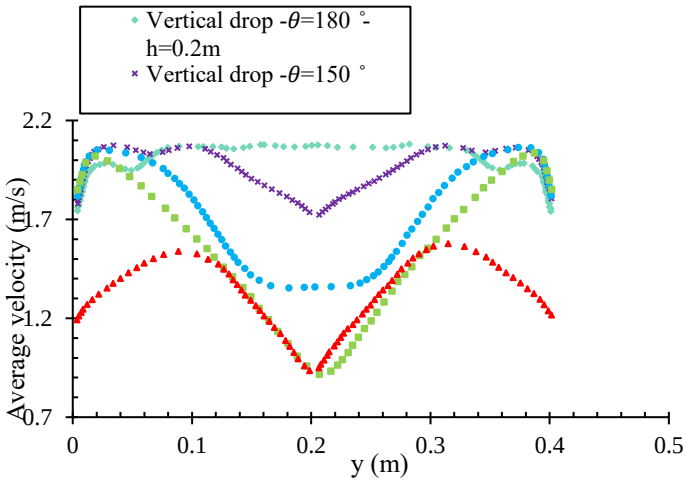

c) Average velocity downstream of the drop

Fig. 16 Comparison of average velocity at different vertex angles

plain vertical drop at two heights. According to Fig. 15, the lowest average velocity corresponds to the foot of the drop where the pool is formed at the vertex angle. The pool causes the jet stream to hit the water instead of the bottom of the channel and reduce its velocity.

The velocity upstream of the drop is slightly higher than the velocity at the foot of the drop, which is also normal, because at the foot of the drop, the pool has reduced the velocity. Downstream of the drop, due to the lack of obstacles in the way of the flow, the water continues on its way and accelerates. The high velocity downstream of the drop is not desirable because it may cause damage. As shown in Fig. 15-c and d, which are related to the drop with a vertex angle of 60 degrees and heights of 0.15 and 0.2 m, it can be seen that by angling the edge of the drop, the downstream velocity decreases. The average velocity downstream of the drop in the middle of the channel, i.e. where the vertex angle is located, has decreased more than at the sides of the channel, i.e. where the wings are located. The average velocities at the foot of the drop in Fig. 15-c and d are also low in the middle of the channel and higher on the sides. In general, it is higher than the average velocity downstream of the drop, and the average velocity upstream of the drop is the lowest. In Fig. 15-e, f, and g which show the average velocity in the vertical drop with vertex angles of 90, 120 and 150 degrees, the average velocity downstream of the drop for all three angles is higher than the average velocity in the other two sections. This means that the only angle where the average velocity has decreased compared to other sections is the 60 degree angle. Regarding the average velocity at the foot of the drop, it can be said that at angles of 90, 120 and 150 degrees the middle of the channel has a lower velocity than the velocity of upstream and on the sides and the average velocity at the foot of the drop is higher than the average velocity upstream on the sides.

Figure 16 compares the average velocity in each of the sections in five drop modes. Figure 16-a shows that the average velocity upstream of the drop in the case of a plain and triangular plan form vertical drops are very close to

each other. The average velocity at the foot of the drop can also be seen in Fig. 16-b which indicates that the velocity at the foot of the drop is the lowest in the plain state and increases with the decrease in the angle because the decrease in the angle causes the depth to decrease. It is pooled and therefore the velocity increases with the decrease of the angle. Downstream of the drop (Fig. 16-c), the plain mode has a higher velocity and the velocity has also decreased with the decrease of the angle.

4. CONCLUSION

In the present research, the hydraulic parameters of a vertical drop with two heights 0.15 and 0.2 m, the vertex angles of 180, 150, 120, 90 and 60 degrees and a flow range of 0.021 to 0.0568 m^3/s was investigated Among the investigated hydraulic parameters, energy dissipation, relative pool depth, relative brink depth, relative downstream depth and average velocity in different sections of the channel were found. By reducing the vertex angle of the drop from 180 degrees to 150, 120, 90 and 60 degrees the energy dissipation increases. The greatest energy dissipation in the 0.2 m drop and an angle of 60 degrees is 64.3%. Reducing the angle has increased the length of the drop wing which means that the length of the water drop has increased and the pool depth at the foot of he drop has decreased; as a result, energy dissipation has increased. Among the vertex angles of the drop, the angle of 60 degrees at the height of the drop of 0.2 m has increased the Froude number from the range of 2.8-3.7 to 0.9-1.5, which is the lowest range of the Froude number. With the reduction of the vertex angle, the relative brink depth at the angle vertex decreases, but at the wings, the relative brink depth is almost equal to the case of a drop with an brink without an angle. The lowest relative brink depth is in the drop with a height of 0.2 m and at an angle of 60 degrees The relative pool depth decreases with the decrease of the angle, and the drop with a height of 0.2 m at an angle of 60 degrees has the lowest relative pool depth. The relative depth of the downstream increases with the decrease of the angle of the brink. The maximum relative downstream depth in the vertical drop with an angled brink was 213% compared to the relative depth of the plain vertical drop, at an angle of 60 degrees and a height of 0.2 m. In examining the average velocity upstream of the channel, angling the edge of the drop has no effect on it, but the average velocity at the foot of the plain drop has the lowest value at both heights of the drop because the pool is the deepest in this area. When the drop brink is angled, the velocity in the middle and the sides of the channel is different, so that the average velocity in the middle becomes lower than the velocity at the sides. As a result, by decreasing the angle, the average velocity at the foot of the drop increases. The maximum average velocity in the downstream is for a plain vertical drop, which gradually decreases with the decrease of the velocity angle in the downstream, so this decrease is more intense in the middle of the channel than on the sides. The structure investigated in the present research can be effective in reducing the construction time of the breakwater with high energy consumption and without additional structure, and also the triangular plan breakwater occupies little space compared to the breakwater with additional structure. In the following, it is suggested that in future studies, the effect of different geometries of the brink drop should be evaluated and compared with the present study. Also, the effect of the creation of supercritical flow in the upstream on the hydraulic parameters was investigated and compared with the subcritical flow. Using an additional structure such as a screen at the same time as changing the geometry of the edge of the drop is another thing that can be done in the future.

CONFLICTS OF INTEREST

The authors declare that they have no conflict of interests.

REFERENCES

Abbaszadeh, H., Norouzi, R., Sume, V., Kuriqi, A., Daneshfaraz, R., & Abraham, J. (2023). Sill Role Effect On The Flow Characteristics (Experimental And Regression Model Analytical). *Fluids*, *8*(8), 235. https://doi.org/10.3390/fluids8080235

Bagherzadeh, M., Mousavi, F., Manafpour, M., Mirzaee, R., & Hoseini, K. (2022). Numerical Simulation And Application Of Soft Computing In Estimating Vertical Drop Energy Dissipation With Horizontal Serrated Edge. *Water Supply*, *22*(4), 4676-4689. https://doi.org/10.2166/Ws.2022.127

Bakhmeteff, B. A. (1932). *Hydraulics of open channels*. ISBN 0 7506 5978 5.

Chamani, M. R., & Beirami, M. K. (2002). Flow Characteristics At Drops. *Journal Of Hydraulic Engineering*, *128*(8), 788-791. https://doi.org/10.1061/(ASCE)0733-9429(2002)128:8(788)

Chamani, M. R., Rajaratnam, N., & Beirami, M. K. (2008). Turbulent Jet Energy Dissipation At Vertical Drops. *Hydraulic Engineering*, *134*, 1532-1535. https:/doi.org/10.1061/(ASCE)0733-9429(2008)134:10(1532)

Crispino, G., Dorthe, D., Gisonni, C., & Pfister, M. (2023). Hydraulic Capacity Of Bend Manholes For Supercritical Flow. *Journal Of Irrigation And Drainage Engineering*, *149*(2), 04022048. https://doi.org/10.1061/JIDEDH.IRENG-10014

Daneshfaraz, R., Bagherzadeh, M., Esmaeeli, R., Norouzi, R., & Abraham, J. (2021a). Study Of The Performance Of Support Vector Machine For Predicting Vertical

Drop Hydraulic Parameters In The Presence Of Dual Horizontal Screens. *Water Supply*, *21*(1), 217-231. https://doi.org/10.2166/ws.2020.279

Daneshfaraz, R., Hasannia, V., Norouzi, R., Sihag, P., Sadeghfam, S., & Abraham, J. (2021b). Investigating The Effect Of Horizontal Screen On Hydraulic Parameters Of Vertical Drop. *Iranian Journal Of Science And Technology, Transactions Of Civil Engineering*, *45*, 1909-1917. https://doi.org/10.1007/S40996-020-00572-W

Daneshfaraz, R., Hasanniya, V., & Norouzi, R. (2022a). Numerical Investigation Of Hydraulic Characteristics Effective On Vertical Drop. *Numerical Methods In Civil Engineering*, *7*(1), 1-8. https://doi.org/10.52547/NMCE.2021.367

Daneshfaraz, R., M. Majedi Asl · S. Razmi · R. Norouzi · J. Abraham (2020). Experimental Investigation Of The Effect Of Dual Horizontal Screens On The Hydraulic Performance Of A Vertical Drop. *International Journal Of Environmental Science And Technology*. 17, 2927–2936. https://doi.org/10.1007/S13762-019-02622-X

Daneshfaraz, R., Norouzi, R., Patrick Abraham, J., Ebadzadeh, P., Akhondi, B., & Abar, M. (2023a). Determination Of Flow Characteristics Over Sharp-Crested Triangular Plan Form Weirs Using Numerical Simulation. *Water Science*, *37*(1), 211-224. https://doi.org/10.1080/23570008.2023.2236384

Daneshfaraz, R., Sadeghfam, S., & Hasanniya, V. (2019). Experimental Investigation Of Energy Dissipation In Vertical Drops Equipped With A Horizontal Screen Under Supercritical Flow. *Iranian Journal Of Soil And Water Research*, *50*(6), 1421-1436. https://doi.org/10.22059/IJSWR.2019.269301.668053

Daneshfaraz, R., Sadeghfam, S., Hasanniya, V., Abraham, J., & Norouzi, R. (2022b). Experimental Investigation On Hydraulic Efficiency Of Vertical Drop Equipped With Vertical Screens. *Teknik Dergi*, *33*(5), 12379-12399. https://doi.org/Https://Doi.Org/10.18400/Tekderg.755938

Daneshfaraz, R., Sadeghfam, S., & Rezazadeh Judi, A. (2017). Laboratory Investigation Of The Influence Of The Location Of Screens On The Amount Of Energy Dissipation. *Engineering Research Of Irrigation And Drainage Structures*, *17*(67), 47-62. (In Persian). https://doi.org/10.22092/Aridse.2017.109616

Daneshfaraz, R., Santos, C. A. G., Norouzi, R., Kashani, M. H., Amirrahmani, M., & Band, S. S. (2023b). Prediction Of Drop Relative Energy Dissipation Based On Harris Hawks Optimization Algorithm. *Iranian Journal Of Science And Technology, Transactions Of Civil Engineering*, *47*(2), 1197-1210. https://doi.org/10.1007/s13201-019-1032-7

Denli Tokyay, N., & Yildiz, D. (2007). Characteristics Free Overfall For Supercritical Flows. *Canadian Journal of Civil Engineering*, *34*, 162-169. https://doi.org/10.1139/L06-114

Esen, I., Alhumoud, J. M., & Hannan, K. A. (2004). Energy Loss At A Drop Structure With A Step At The Base. *Water International*, *29*, 523 - 529. https://doi.org/10.1080/02508060408691816

Gill, M. A. (1979). Hydraulics Of Rectangular Vertical Drop Structures. *Journal Of Hydraulic Research*, *17*(4), 289-302. https://doi.org/10.1080/00221687909499573

Helmi, A. M., Essawy, H. T., & Wagdy, A. (2019). Three-Dimensional Numerical Study Of Stacked Drop Manholes. *Journal Of Irrigation And Drainage Engineering*, *145*(9), 04019017. https://doi.org/10.1061/(ASCE)IR.1943-4774.0001414

Hong, Y. M., Huang, H. S., & Wan, S. (2010). Drop characteristics of free-falling nappe for aerated straight-drop spillway. *Journal Of Hydraulic Research*, *48*(1), 125-129. https://doi.org/10.1080/00221680903568683

Liu, S. I., Chen, J. Y., Hong, Y. M., Huang, H. S., & Raikar, R. V. (2014). Impact characteristics of free over-fall in pool zone with upstream bed slope. *Journal of Marine Science and Technology*, *22*(4), 476-486. https://doi.org/10.6119/JMST-013-0604-1

Moore, W. L. (1943). Energy Loss at the base of a free overfall. *Transactions of the American Society of Civil Engineers*, *108*(1), 1343-1360.

Norouzi, R., Sihag, P., Daneshfaraz, R., Abraham, J., & Hasannia, V. (2021). Predicting relative energy dissipation for vertical drops equipped with a horizontal screen using soft computing techniques. *Water Supply*, *21*(8), 4493-4513. https://doi.org/10.2166/ws.2021.193

Rand, W. H. (1955). Flow Geometry at straight drop spillways. *Environmental Science*, *81*(9), 1-13.

Torres, C., Borman, D., Sleigh, A., & Neeve, D. (2021). Application of three-dimensional CFD VOF to characterize free-surface flow over trapezoidal labyrinth weir and spillway. *Journal of Hydraulic Engineering*, *147*(3), 04021002. https://doi.org/10.1061/(ASCE)HY.1943-7900.000185

White, M. P. (1943). Discussion of moore (1943). *ASCE*, *108*, 1361-1364.

Yonesi, H. A., Daneshfaraz, R., Mirzaee, R., & Bagherzadeh, M. (2023). Maximum energy loss in a vertical drop equipped with horizontal screen with downstream rough and smooth bed. *Water Supply*, *00*. https://doi.org/10.2166/ws.2023.005

Zahabi, H., Torabi, M., Alamatian, E., Bahiraei, M., & Goodarzi, M. (2018). Effects of geometry and hydraulic characteristics of shallow reservoirs on sediment entrapment. *Water*, *10*(12), 1725. https://doi.org/10.3390/w10121725